Protein kinase CK2 is involved in zinc homeostasis in breast and prostate cancer cells

Mohammad S. Zaman · Adam J. Johnson · Gayani Petersingham · Gerald W. Muench · Qihan Dong · Ming J. Wu

Abstract The intracellular zinc profiles of breast and prostate cancer cells are diametrically opposed, with hyper-accumulation of zinc in breast cancer, and low level in prostate cancer. This phenomenon is poorly understood. This study employs two breast and two prostate cancer cell lines to investigate the role of protein kinase CK2 in regulating zinc homeostasis. CK2 was targeted by its specific inhibitors 4,5,6,7-tetrabromobenzotriazole (TBB) and CX-4945, and by the specific siRNA against each of the three CK2 genes. The effect of zinc exposure after the above CK2 manipulation was observed by MTT [3-(4,5-dimethyliazol-2-yl)-2,5-diphenyl-2H-tetrazolium bromide] cell viability assay and confocal microscopy for intracellular zinc level. The results demonstrate that CK2 is involved in regulating zinc homeostasis in breast and prostate cancer cells as both TBB and CX-4945 substantially decreased cell viability upon zinc exposure. siRNA-mediated knockdown of the three CK2 subunits (α, α' and β) revealed their discrete roles in regulating zinc homeostasis in breast and prostate cancer cells. Knockdown of CK2α' decreased the intracellular zinc level of breast cancer cells and in turn increased the cell viability while the opposite findings were obtained for the prostate cancer cells. Knockdown of CK2β expression substantially increased the zinc level in breast cancer cell lines whilst decreased the zinc level in prostate cancer cells. Taken together, this study shows that CK2 is involved in zinc homeostasis of breast and prostate cancer cells and opens a new avenue for research on these cancers.

Keywords Zinc homeostasis · Protein kinase CK2 · Breast cancer · Prostate cancer

M. S. Zaman · A. J. Johnson · G. Petersingham · Q. Dong · M. J. Wu (✉)
School of Science and Health, Western Sydney University, Locked Bag 1797, Penrith, NSW 2751, Australia
e-mail: m.wu@westernsydney.edu.au

G. W. Muench
Pharmacology Unit, School of Medicine, Western Sydney University, Locked Bag 1797, Penrith, NSW 2751, Australia

M. J. Wu
Molecular Science Research Group, School of Medicine, Western Sydney University, Locked Bag 1797, Penrith, NSW 2751, Australia

Introduction

The ubiquitous and pleiotropic serine/threonine protein kinase CK2 (CK2) was first discovered by Burnett and Kennedy in 1954 (Burnett and Kennedy 1954). Its structural and functional characteristics have since been catalogued (Litchfield 2003; Meggio and Pinna 2003; Pinna 1993). Structurally, the mammalian CK2 heterotetramer is composed of two catalytic

subunits (α and α') and a homodimer of regulatory β subunits (Bischoff et al. 2011; Niefind et al. 2001). Homodimerisation of the β subunits requires two zinc ions which are held by the zinc fingers, essential for dimer formation (Chantalat et al. 1999). Monomeric CK2 α and α' subunits are also catalytically active in the absence of the β subunit (Niefind et al. 2001; Raaf et al. 2008). Functionally, CK2 plays roles in cell proliferation, differentiation and apoptosis, therefore it is implicated in diseases such as cancers (Guerra et al. 1999; Guerra and Issinger 1999; Litchfield 2003). CK2 has been regarded as the most pleiotropic kinase in eukaryotic organisms due to its numerous substrates which possibly make up one quarter of the eukaryotic phosphoproteome (Litchfield 2003; Meggio et al. 1994; Meggio and Pinna 2003; Pinna 1993). Despite such enormous progress in the characterisation of CK2, many aspects of its function remain yet to be fully elucidated such as its role in regulating zinc homeostasis in cancer cells.

Zinc is arguably one of the most important biometal ions in living organisms, involved in a range of biological functions such as being a cofactor for enzymes, a structural component of proteins and a second messenger for signalling pathways (Hershfinkel et al. 2001; Laity et al. 2001; Maret 2001; Taylor et al. 2012). It is estimated that there are at least 3000 zinc-binding proteins in the human proteome (Maret 2012). About 40% of those proteins are transcription factors which often contain zinc-finger motifs allowing the proteins to coordinate zinc ions for the formation of essential structures in DNA binding (Ebert and Altman 2008). The zinc level is highly regulated in the cell because of its diverse functions (Vallee and Auld 1990). Such regulation involves its uptake, sequestration and efflux (Guerinot 2000; Yamasaki et al. 2007). There are two groups of zinc transport proteins including 10 ZnT (zinc transporters) for decreasing the cytoplasmic zinc level ($[Zn^{2+}]$), and 14 ZIP (ZRT/IRT-like proteins) for increasing the cytoplasmic $[Zn^{2+}]$ (Cousins et al. 2006; Guerinot 2000). Metallothioneins are also involved in maintaining the homeostasis of $[Zn^{2+}]$ (Suhy et al. 1999). Dysregulation of zinc homeostasis is linked to cancers (Costello and Franklin 2006). Breast cancer cells have been shown to have a higher $[Zn^{2+}]$ compared to normal mammary epithelial cells (Alam and Kelleher 2012). This increased Zn^{2+} level is correlated with higher malignancy of the cancer (Kagara et al. 2007).

In clear contrast, Zn^{2+} level is significantly decreased in prostate cancer cells compared to normal prostate cells (Franklin et al. 2005; Song and Ho 2009). Such diametrically opposite profiles of zinc in these two types of cancer cells serve as an ideal tool for this study to dissect the role of CK2 in regulating zinc homeostasis.

CK2 is found to regulate zinc uptake and sequestration in eukaryotic cells. We, using the model organism *Saccharomyces cerevisiae*, discovered that CK2α subunit is involved in Zn^{2+} sequestration (Johnson et al. 2017). We further demonstrated that CK2 plays a role in Zn^{2+} uptake and toxicity in neuronal cells (Zaman et al. 2016). Taylor et al. (2003) showed CK2 phosphorylates the zinc channel ZIP7 located in the membrane of endoplasmic reticulum, allowing Zn^{2+} to be released into the cytoplasm. All these previous findings provide a basis for this study, which is to investigate the role of CK2 in zinc homeostasis in breast and prostate cancer cells. Our experimental approach is to target CK2 with its specific inhibitors at the protein level and its specific siRNA at the gene level in breast cancer cell lines (MCF-7 and MDA-MB-231) and prostate cancer cell lines (PC3 and DU145). The effects of such CK2 manipulation in combination with zinc exposure are then observed by MTT cell viability assay and confocal microscopy for intracellular zinc level quantification. The findings reported below provide evidence for the involvement of CK2 in zinc homeostasis of breast and prostate cancer cells.

Materials and methods

Culturing conditions

MCF-7 cells (human breast adenocarcinoma, ATCC Cat. No. ATCC® HTB-22™) and DU145 cells (human prostate cancer, ATCC Cat. No. ATCC® HTB-81™) were cultured in DMEM (Life Technologies, Australia) supplemented with 10% foetal bovine serum (FBS) (Life Technologies, Australia), 1% antibiotics (penicillin/streptomycin) (Life Technologies, Australia), and L-glutamine. MDA-MB-231 cells (human breast cancer, ATCC Cat. No. ATCC® CRM-HTB-26™) were cultured in Leibovitz's L-15 medium (Life Technologies, Australia) supplemented with 10% FBS, 1% antibiotics and L-glutamine. PC3 cells

(human prostate cancer, ATCC Cat. No. ATCC® CRL-1435™) were cultured in RPMI 1640 (Life Technologies, Australia) supplemented with 10% FBS, 1% antibiotics and L-glutamine. Cells were incubated at 37 °C with 5% CO_2 and observed daily until 80% confluence. The cells were then washed with phosphate-buffered saline (PBS), trypsinised, counted using a haemocytometer (LW Scientific) and seeded into appropriate flasks or plates for experimentation.

MTT assay and cell enumeration

Cells were seeded into 96-well plates (Greiner Bio-one) in 190 µL complete medium containing 7000 cells per well. Plates were incubated at 37 °C and 5% CO_2 for 32 h before treatment with $ZnSO_4$. Stock solutions of $ZnSO_4$ were made at 20X concentrations and filter-sterilised through a 0.22 µm filter. The final concentrations of $ZnSO_4$ used were 0, 20, 50, 100, 150, 200, 250, 300, 350, 400 and 500 µM. After treatment with $ZnSO_4$, plates were incubated for 6 h and then treated with 50 µL/well of MTT [3-(4,5-dimethyliazol-2-yl)-2,5-diphenyl-2H-tetrazolium bromide, 5 mg/mL in PBS], followed with a further incubation of 2 h at 37 °C in 5% CO_2 incubator. The medium was then aspirated and formazan crystals in each well were solubilised in 100 µL of dimethyl sulfoxide (DMSO). Plates were then shaken gently before the optical absorbance was measured at 600 nm (A_{600}) using a spectrophotometer (Multiskan EX, Thermo Electron). The cell viability was quantified from the collected data and the AAT Bioquest website (https://www.aatbio.com/tools/ic50-calculator) was used to generate IC_{50} values and further confirmed by graphing through Excel.

For cell enumeration, the cells were grown, prepared and treated in the same way as described previously. Following the 6 h incubation of $ZnSO_4$ treatments, the medium from each 96-well plate was aspirated and wells were washed with 200 µL of PBS, trypsinised with 15 µL of trypsin and then incubated for 2–3 min at 37 °C in 5% CO_2 incubator. Then 185 µL of medium was pipetted into each well, cells were thoroughly re-suspended and transferred to microcentrifuge tubes. Equal volume of 0.4% trypan blue (Life Technologies) dye was added to each tube and thoroughly mixed by pipetting prior to cell counting with a haemocytometer under a light microscope (Olympus CHX41). Both live and dead cells were counted to calculate the percentage of viable cells. Cell viability was graphed using the Bioquest website for IC_{50} determination and further confirmed through graphing in Excel.

CK2 inhibition and zinc treatment

Multiple 96-well plates were prepared containing 7000 cells per well in 190 µL of complete medium and incubated for 32 h. Prior to the addition of $ZnSO_4$, cells were treated with CK2 specific inhibitor TBB (4,5,6,7-tetrabromo-1H-benzotriazole, Calbiochem-Millipore) or CX-4945 (Adooq Bioscience) dissolved in DMSO. A final concentration of 20 µM TBB and 5 µM CX-4945 was used for CK2 inhibition. This dose for each inhibitor was chosen on the basis of its benign toxicity based on a titration we preformed and further supported by literature (Cozza et al. 2009; Zaman et al. 2016; Zwicker et al. 2011). After the addition of TBB or CX-4945, the cells were incubated at 37 °C with 5% CO_2 for 3 h, followed by 6 h incubation of $ZnSO_4$ at IC_{50}. At the end of the incubation period, plates were observed under the microscope and the cell viability was measured by MTT assay as described earlier.

CK2 knockdown and zinc treatment

SMARTpool siRNA targeting the individual genes of CK2 subunits (CSNK2A1 encoding CK2α, CSNK2A2 encoding CK2α′ and CSNK2B encoding CK2β) were purchased from Dharmacon, USA. Each SMARTpool siRNA against a specific subunit gene is comprised of four targeting nucleotides. The targeting sequences for CSNK2A1 were UGAAUUAGAUCCACGUUUC, GCAAUUGUACCAGACGUUA, CAGAAAGCUU CGGCUAAUA, AGACUAUGACAUUCGAUUU. The targeting sequences for CSNK2A2 were GCAA-GUAUAGUGAAGUAUU, CAACAGAGAUU-GACCGCCA, GGUGGAACAAAUAUCAUUA, GAACUAUAUGGUUAUCUGA. The targeting sequences for CSNK2B were CAGCUGAGAUG-CUUUAUGG, CCAAGUGCAUGGACGUGUA, GGUAAUGAAUUCUUCUGUG, GCAGGGAGA-CUUUGGCUAC. Each SMARTpool siRNA stock (10 µM) was prepared in siRNA buffer (pH 7.3) containing 300 mM potassium chloride, 31 mM HEPES and 2.1 mM magnesium chloride. For each siRNA transfection, two microcentrifuge tubes were

prepared, with tube 1 containing 20 μL of 10 μM siRNA and 480 μL OPTI-MEM (Life Technologies) and tube 2 containing 20 μL lipofectamine 2000 (Invitrogen) and 480 μL OPTI-MEM. After 5 min incubation at room temperature, the contents of tube 1 was pipetted into tube 2 for each siRNA and left at room temperature for 20 min. A mock tube with no siRNA containing 980 μL OPTI-MEM with 20 μL lipofectamine was also prepared to serve as a control.

Cells were cultured in flasks for 32 h until 80% confluence. The cells were washed with PBS, then trypsinised and 5 mL fresh complete medium was added. The cells were counted and 2×10^6 cells in 5 mL was prepared for each treatment including CSNK2A1 siRNA, CSNK2A2 siRNA, CSNK2B siRNA and mock control. The cells were centrifuged at $900 \times g$ for 5 min. The supernatant was removed and cells were then washed with 5 mL PBS and centrifuged again with the supernatant discarded. The four treatments were then performed with each cell pellet thoroughly re-suspended in 1 mL of each siRNA mixture prepared previously. After 20 min incubation, 9 mL of OPTI-MEM was added and the cells were then re-suspended and aliquoted into 96-well plates at 95 μL per well. The plates were incubated at 37 °C in 5% CO_2 incubator for 36 h. The IC_{50} of $ZnSO_4$ in 5 μL volume per well were used to treat the transfected cells in the plates and incubated at 37 °C in 5% CO_2 incubator for 6 h. An MTT assay was then conducted to measure cell viability as previously described.

Reverse transcription quantitative PCR (RT-qPCR)

Total RNA samples were prepared from the siRNA treated cells. After siRNA treatment, cells were grown in 25 cm^2 flasks for 36 h. For each treatment, the medium was discarded and 1 mL of TRIzol^{TM} reagent (Thermofisher) added directly into the flask. By pipetting up and down several times the lysate was homogenised and transferred to 2 mL microcentrifuge tubes, followed with 5 min incubation at room temperature. Then, 200 μL of chloroform (Sigma-Aldrich, Australia) was added and the sample was left for 3 min incubation prior to centrifugation at $12,000 \times g$, 4 °C for 15 min to separate into three phases. The RNA containing upper phase was transferred to a new tube and precipitated by adding 0.5 mL of isopropanol (Sigma-Aldrich, Australia). After

10 min incubation the sample was centrifuged for 10 min at $12,000 \times g$, 4 °C. The supernatant was then discarded and the RNA pellet was washed in 1 mL 75% ethanol (Sigma-Aldrich) by vortexing for 5 s then centrifugation for 5 min at $7500 \times g$, 4 °C. The resultant pellet was allowed to air dry for about 20 min and then reconstituted in 30 μL RNase-free water (Sigma-Aldrich, Australia) and stored at $- 80$ °C (Thermo Scientific $-$ 80C ULT). Quantification and determination of RNA purity was accomplished by measuring the UV absorbance (A_{260}, A_{280}, A_{260}/A_{280}).

cDNA was synthesised using high-capacity cDNA reverse transcription kits (Thermo Fisher Scientific) according to the manufacturer's instructions. Firstly 10 μL of master mix was prepared with 2 μL 10X reverse transcription buffer, 0.8 μL 25X dNTP mix, 2 μL 10X reverse transcription random primers, 1 μL Multiscribe^{TM} reverse transcriptase, and 4.2 μL DEPC treated water. Then, 10 μL of the master mix was combined with 10 μL of 0.1 μg/μL total RNA from a specific siRNA treatment. The reaction tube was mixed and then run on a Veriti 96-well thermal cycler (Applied Biosystems) with the following thermal cycler settings: step 1 at 25 °C for 10 min, step 2 at 37 °C for 120 min, step 3 at 85 °C for 5 s. cDNA synthesis was quantified by measuring the UV absorbance (A_{260}, A_{280}, A_{260}/A_{280}).

qPCR was carried out using TaqMan real time PCR reagents (Thermo Fisher Scientific) according to the manufacturer's instructions. Each 20 μL reaction mix contained 1 μL 20X TaqMan assay which contains specific primer/probe combinations for a CK2 gene, 10 μL master mix, 1 μL of cDNA template (500 ng/μL) and 8 μL DEPC treated water (9 μL for the no template control). Each cDNA was run in triplicate. The mixture was heated at 95 °C for 10 min, then followed with each cycle at 95 °C for 15 s and at 60 °C for 1 min, for 40 cycles. The relative expression of CK2 genes (CSNK2A1, CSNK2A2 and CSNK2B) against the house keeping gene GAPDH (glyceraldehyde-3-phosphate dehydrogenase) was quantified.

Data generated were analysed by the $2^{-\Delta\Delta CT}$ method (Schmittgen and Livak 2008). ΔCTc is calculated first where the cycle threshold for the gene of interest in control conditions was normalised to the cycle threshold of the house keeping gene GAPDH control in mock condition. Then the cycle threshold of the gene of interest under each treatment was normalised to the cycle threshold of GAPDH under
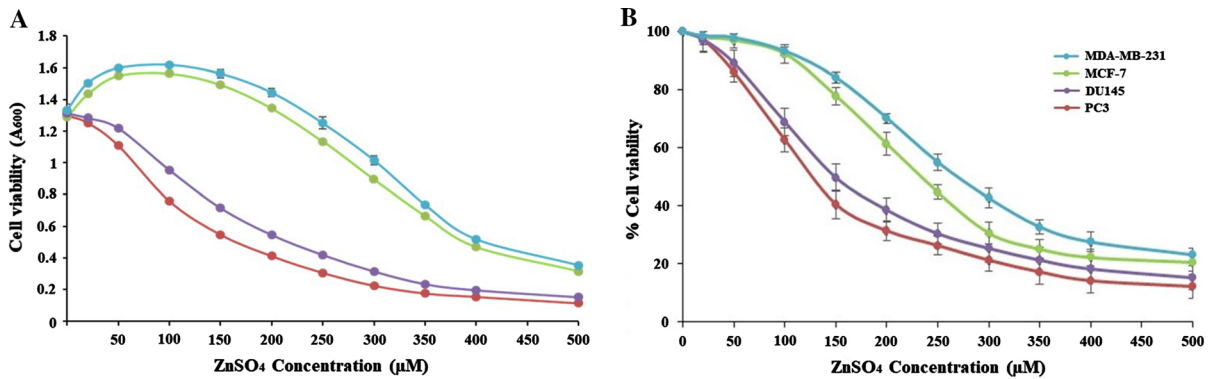
Fig. 1 Determination of IC_{50} of $ZnSO_4$ by MTT assay (**a**) and by cell counting (**b**). IC_{50} of $ZnSO_4$ at 6 h for all four cancer cell lines was determined by MTT assay. IC_{50} for MCF-7 cells (green) is 320 μM, MDA-MB-231 cells (blue) 350 μM, PC3 cells (red) 110 μM and DU145 cells (purple) 150 μM (**a**). The trend observed by MTT assay was confirmed by cell counting using trypan blue (**b**). Error bars denotes standard deviation of three biological replicates for each dose. (Color figure online)

each experimental treatment (ΔCTe). Finally, the ratio of ΔCTe over ΔCTc is ΔΔCT. The expression of fold change is given by $2^{-\Delta\Delta CT}$.

Confocal microscopy imaging

Confocal imaging glass bottom culture dishes (Greiner Bio-One) were firstly coated with 20 μL of gelatin (Sigma-Aldrich, Australia) on the glass surface. Cells suspended in complete medium with 25 mM HEPES buffer were seeded at 40,000 cells per mL into each imaging dish at a final volume of 1 mL. Cells were incubated at 37 °C in 5% CO_2 incubator for 32 h. The cells were treated as previously described with CK2 inhibitor TBB (20 μM) or CX-4945 (5 μM) or the specific siRNAs against each CK2 subunit gene. IC_{50} $ZnSO_4$ was applied for 1 h before the removal of medium and addition of 1 mL fresh live cell imaging medium (Life Technologies) containing 140 mM NaCl, 2.5 mM KCl, 1.8 mM $CaCl_2$, 1 mM $MgCl_2$ and 20 mM HEPES at pH 7.4. The zinc probe stock was prepared by dissolving 100 μg of FluoZin-3 AM in 198 μL of DMSO and 2 μL of 50% pluronic acid F127, followed by 5 min sonication. To each culture dish 15 μL of FluoZin-3 AM stock was added. After a further 1 h incubation at 37 °C in 5% CO_2 incubator, the medium was removed and 2 mL of fresh imaging medium was added and incubated at 37 °C in 5% CO_2 for 30 min prior to imaging. Confocal imaging was performed in all four cell lines. Images were acquired using an LSM-5 Confocal Microscope system (Carl Zeiss Pty Ltd, North Ryde, Australia), with excitation

at 488 nm and emission at 510–530 nm. Gain settings for fluorescence imaging were maintained constant for the imaging probe to allow for quantification of intracellular fluorescence intensity through Image-J imaging software.

Statistical analysis

Data was analysed with one-way ANOVA in SPSS statistical software. Analysis and quantification of confocal images was achieved via Image-J with Fiji attachment software.

Results

IC_{50} of $ZnSO_4$ in the cancer cell lines

In order to measure the effect of zinc on the cancer cells, its IC_{50} for each cancer cell line was firstly determined by MTT assay. As shown in Fig. 1, the overall patterns for the breast cancer cell lines (MCF-7 and MDA-MB-231) and prostate cancer cell lines (PC3 and DU145) in response to the zinc exposure are divergent. The IC_{50} values of $ZnSO_4$ for MCF-7 (320 μM) and MDA-MB-231 (350 μM) are much higher than that of PC3 (110 μM) and DU145 (150 μM) (Fig. 1a). These IC_{50} values are used in the following experiments. For each cell line the IC_{50} of $ZnSO_4$ was also determined via cell counting, which confirms the trend observed by MTT assay as shown in Fig. 1b.
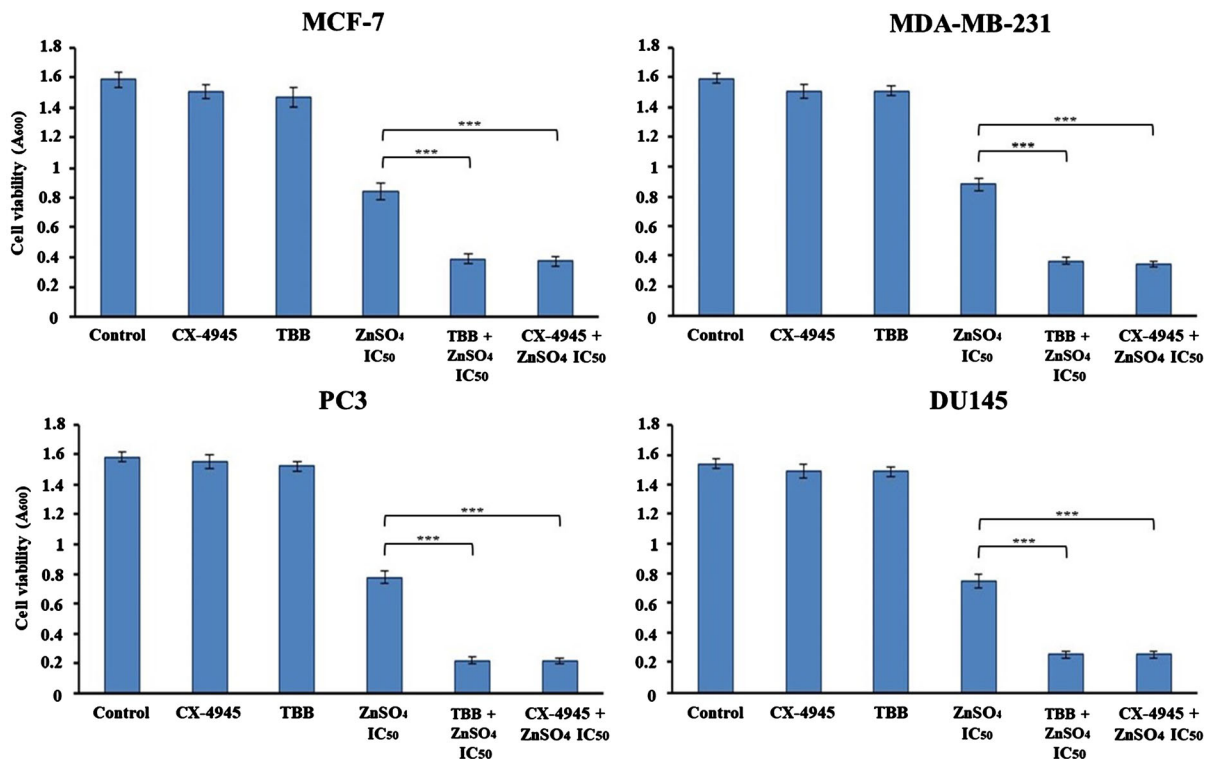
Fig. 2 Effect of CK2 inhibitors on cancer cell viability under exposure of IC_{50} $ZnSO_4$. Cells were treated with 20 μM TBB or 5 μM CX-4945 inhibitor for 3 h and then incubated for 6 h with the IC_{50} of $ZnSO_4$. The cell viability was determined by MTT assay. Error bars denotes standard deviation of three biological replicates for each treatment and each biological replicate has three technical replicates. P values were calculated by one-way ANOVA. ***$P < 0.001$

Effect of CK2 inhibitors on Zn^{2+} homeostasis under exposure of IC_{50} $ZnSO_4$

To uncover the role of protein kinase CK2 in regulating zinc homeostasis, the specific inhibitors TBB and CX-4945 were used. As shown in Fig. 2, CK2 inhibitor alone with TBB (20 μM) or CX-4945 (5 μM) had little effect on the cancer cell viability. The inhibitor plus IC_{50} of $ZnSO_4$ reduced the viability of both breast (MCF-7, MDA-MB-231) and prostate (PC3, DU145) cancer cells ($P < 0.001$), and prostate cancer cells exhibiting higher sensitivity to the treatment of CK2 inhibitor plus zinc exposure.

Efficacy of CK2 gene expression knockdown by siRNA

Relative expression of CK2 subunit genes (CSNK2A1, CSNK2A2 and CSNK2B) was determined with reference to the expression of housekeeping gene GAPDH. Fold change 1 means no change of the gene expression. Fold change > 1 means increase of the gene expression whilst fold change < 1 means decrease of the gene expression. Figure 3 shows the percentage knockdown of CSNK2A1 (encoding CK2α) is 80.7% for MCF-7, 59.4% for MDA-MB-231, 58.7% for PC3 and 65.7% for DU145 cells. The percentage knockdown of CSNK2A2 (CK2α′) is 70.5% for MCF-7, 67.1% for MDA-MB-231, 72.5% for PC3 and 61.4% for DU145 cells. The percentage knockdown of CSNK2B (CK2β) is 78.2% for MCF-7, 75.2% for MDA-MB-231, 76.4% for PC3 and 76% for DU145. In all of the four cell lines, knockdown of one CK2 gene does not affect the other two, except in MCF-7 where knockdown of CK2β leads to reduction in expression of CK2α and α′, and knockdown α′ leads to reduction in expression of β, as well as in DU145, knockdown of α′ caused reduction in expression of α.

MCF-7

MDA-MB-231

PC3

DU145
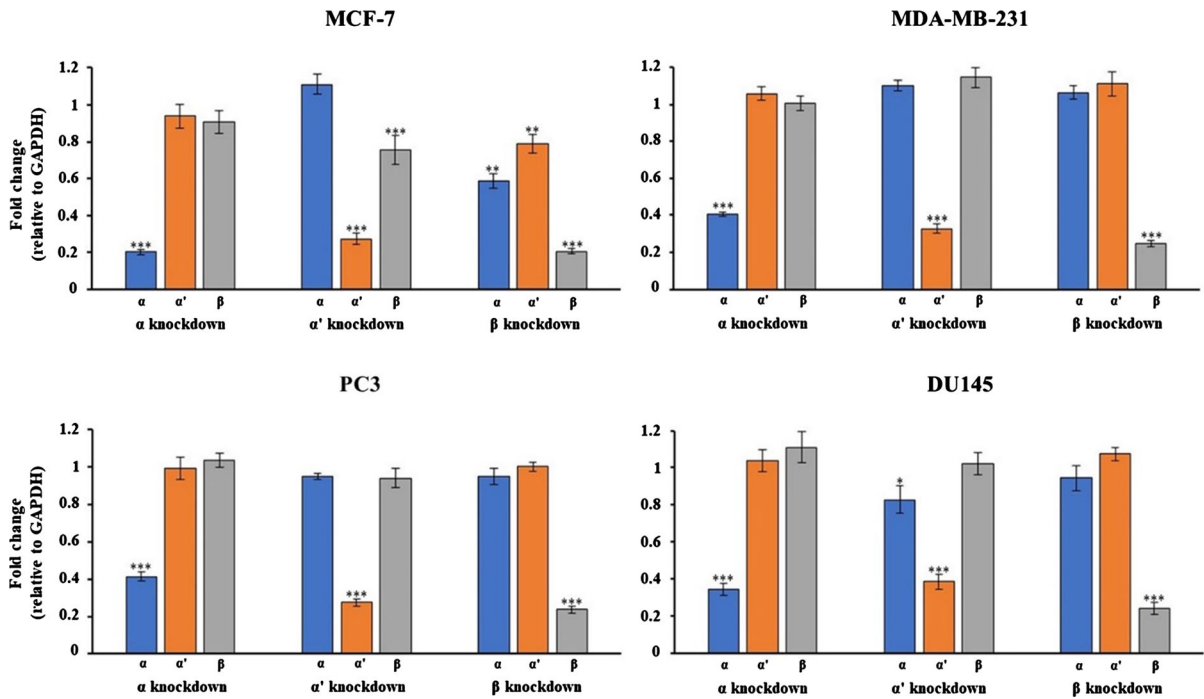
Fig. 3 Efficacy of CK2 gene expression knockdown by the specific siRNA. Cells were transfected with CK2 subunit specific siRNA and incubated for 36 h. Total RNA was then prepared, cDNA synthesised and qPCR performed. Relative expression of the subunit genes was quantified relative to GAPDH. $*P < 0.05$, $**P < 0.01$ and $***P < 0.001$. Data represents the average of three biological replicates and each biological replicate has two technical replicates. Error bars represent SEM. CSNK2A1 is denoted as α, CSNK2A2 as α' and CSNK2B as β

Effect of CK2 siRNA knockdown on cell viability under zinc exposure

The knockdown of individual CK2 subunit genes revealed their distinct involvements in regulating zinc homeostasis reflected by the cancer cell viability (Fig. 4). Compared to mock transfection plus $ZnSO_4$ IC_{50}, knockdown of CK2α increased cell viability of MDA-MB-231 cells ($P < 0.01$) but decreased cell viability in MCF-7, PC3 and DU145 cells ($P < 0.001$). Knockdown of CK2α' increased cell viability of MCF-7 and MDA-MB-231 cells ($P < 0.001$) but decreased cell viability in PC3 and DU145 cells ($P < 0.001$). Knockdown of CK2β decreased cell viability of MCF-7 and MDA-MB-231 cells ($P < 0.001$) but increased cell viability in PC3 ($P < 0.01$) and DU145 cells ($P < 0.001$). Across all three knockdowns, the two prostate cancer cell lines showed consistent effects, the same is also true for the two breast cancer cell lines except the knockdown of CK2α. The discrepancy of the effect
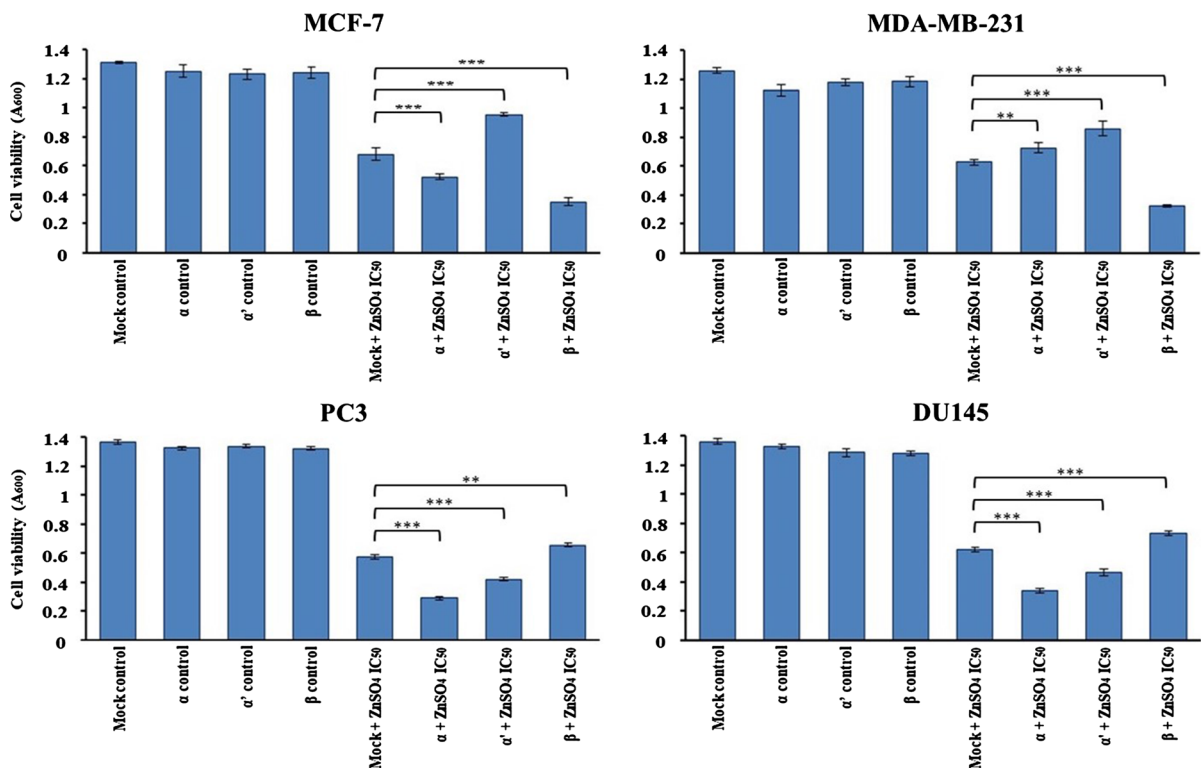
of CK2α knockdown is likely due to the lower knockdown efficacy in MDA-MB-231.

Visualisation of intracellular Zn^{2+} in $ZnSO_4$ treated cells under CK2 inhibition and siRNA knockdown

Apart from performing MTT assays, the effects of CK2 inhibitors and siRNA knockdown in MCF-7, MDA-MB-231, PC3 and DU145 cells were further studied by confocal imaging with the specific fluorophore (FluoZin-3 AM) for zinc visualisation and quantification (Figs. 5, 6). Figure 5 shows that zinc levels in all four cell lines were significantly increased by the inhibition of CK2 inhibitors TBB or CX-4945 in combination with IC_{50} zinc exposure compared to zinc IC_{50} treatment alone ($P < 0.001$). The cells with inhibitor alone (Control panel) and the cells with $ZnSO_4$ only ($ZnSO_4$ panel) serve as controls. Notably, the zinc level in the controls of breast cancer cells is higher than the counterparts of prostate cancer cells,

demonstrating the intrinsic characteristics of these two types of cancer cells.

Visualisation of zinc levels by confocal imaging in the cells transfected with CK2 specific siRNA reveals the distinct involvements between each CK2 subunit and intracellular zinc level (Fig. 6). Under $ZnSO_4$ IC_{50} treatment, knockdown of CK2β is detrimental to both breast cancer cell lines ($P < 0.001$) but is beneficial to both prostate cancer cells ($P < 0.001$), particularly PC3 cells. CK2α′ knockdown reduced the zinc level significantly in MCF-7 and MDA-MB-231 cells ($P < 0.001$), whereas no apparent effect was displayed by PC3 and DU145 cells. Knockdown of CK2α increased the zinc level in PC3 and DU145 cell lines ($P < 0.001$), while such effect was not apparent for MCF-7 and MDA-MB-231 cells. Furthermore, the control images revealed that zinc ions are most likely localised surrounding the nuclei. Such a pattern was also obvious in the cells with CK2α′ knockdown, particularly in MCF-7 and MDA-MB-231 cells.

Fig. 5 Visualisation of Zn^{2+} in $ZnSO_4$ treated cells under CK2 ▶ inhibition. Cells were grown in confocal imaging dishes for 32 h then treated with either TBB (20 μM) or CX-4945 (5 μM) for 3 h followed by $ZnSO_4$ IC_{50} treatment and incubation with the fluorescent probe FluoZin-3 AM. The confocal images (**a**) were taken at ×40 magnification. The control panel represents the cells treated with the CK2 inhibitor alone (either TBB or CX-4945). Fluorescent intensity (**b**) was quantified for each treatment with confocal images at ×40 magnification where blue indicates MCF-7 cells, orange MDA-MB-231 cells, grey PC3 cells and yellow DU145 cells. Error bars denote standard deviation of fluorescence intensity for each treatment. (Color figure online)

Discussion

Zinc hyper-accumulates in breast cancer cells compared to normal mammary epithelial cells (Chandler et al. 2016; Lopez et al. 2011), while prostate cancer cells have much lower zinc content than normal prostate cells (Franklin et al. 2005; Song and Ho 2009). Such phenomenon is poorly understood at a

Fig. 4 Effect of CK2 siRNA knockdown on cell viability under zinc exposure. Transfection of siRNA was carried out in MCF-7, MDA-MB-231, PC3 and DU145 cells, followed by treatment of $ZnSO_4$ IC_{50} and an MTT assay. Mock transfection as well as mock plus $ZnSO_4$ IC_{50} served as two controls. P values were calculated by one-way ANOVA. $**P < 0.01$ and $***P < 0.001$. Error bars denote standard deviation of three biological replicates for each treatment and each biological replicate has two technical replicates
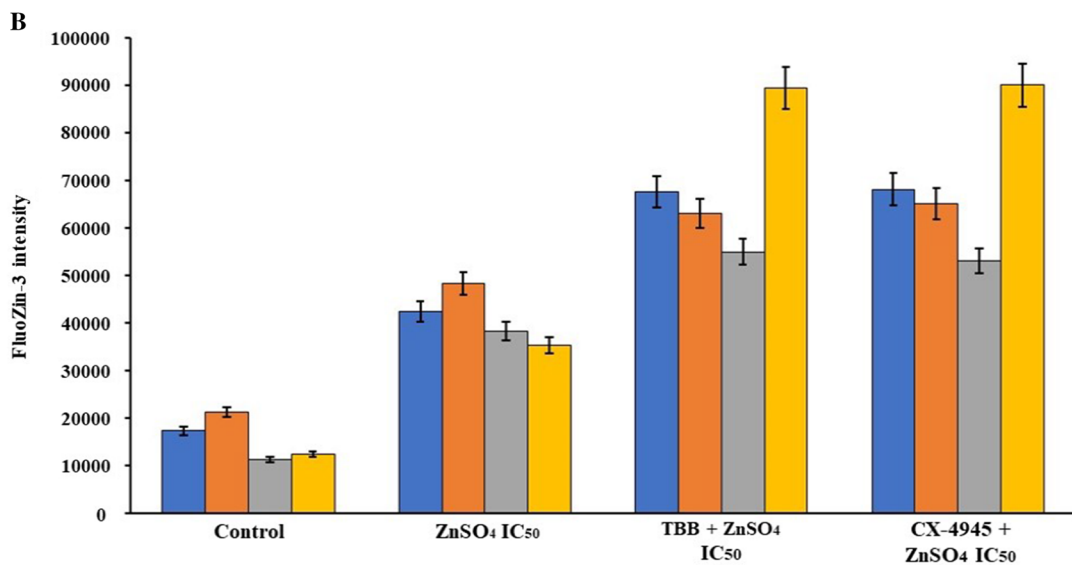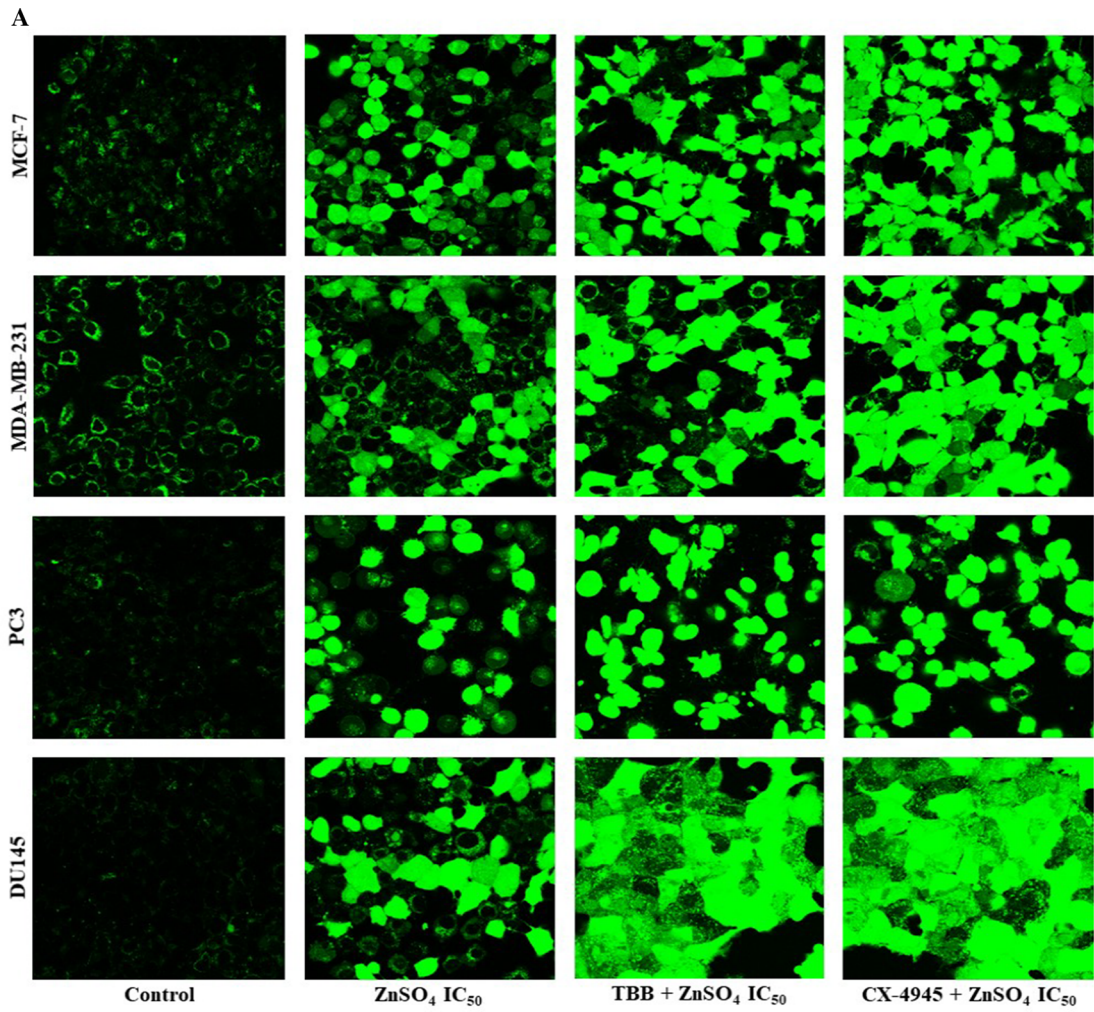
molecular level. By using breast and prostate cancer cells and manipulating protein kinase CK2 at protein and gene levels, this study acquired significant evidence for the involvement of CK2 in zinc homeostasis of breast and prostate cancer cells.

From the response curves of breast and prostate cancer cells against zinc titration (Fig. 1a), a conspicuous divergence between the two types of cancer cells demonstrates that breast cancer cells are more capable of coping with acute zinc exposure than prostate cancer cells. No cytotoxicity is evident up to approximately 150 μM $ZnSO_4$ for breast cancer cells, whilst prostate cancer cells show little tolerance to 20 μM $ZnSO_4$. This is further confirmed by trypan blue staining and cell counting (Fig. 1b). Together with the control images in Figs. 5 and 6, the data supports the known phenomenon, that is, breast cancer cells have a higher zinc content than prostate cancer cells (Alam and Kelleher 2012; Costello and Franklin 2006). The findings reported here provide some insights into this phenomenon in terms of the involvement of CK2.

The cancer cell's response to zinc exposure is underpinned by the regulation of uptake, sequestration and efflux of Zn^{2+}. As described at the outset, there are numerous membrane-bound transport proteins for Zn^{2+}, including 10 ZnT involved in decreasing cytoplasmic zinc level, and 14 ZIP for increasing cytoplasmic zinc (Margalioth et al. 1983; Nelson 1999; Yamasaki et al. 2007). These transporters are either present in the plasma membrane or in the membranes of subcellular organelles such as the endoplasmic reticulum (Cousins et al. 2006; Yamasaki et al. 2007). Their regulation by other molecules such as CK2 (Guerra et al. 1999; Sekler et al. 2007; Taylor et al. 2008; Zaman et al. 2016) and metal regulatory transcription factor (Lopez et al. 2011; Suhy et al. 1999) is critical to maintain the homeostasis of cytoplasmic zinc, which is estimated to be at picomolar levels in eukarya (Bozym et al. 2006; Krężel and Maret 2006; Outten and O'halloran 2001; Vinkenborg et al. 2009).

The experiments using CK2 inhibitors demonstrate that CK2 function is required by both breast and prostate cancer cells to regulate zinc homeostasis under zinc exposure. The reason behind using two inhibitors, TBB and CX-4945, is to enhance the veracity of the findings since no inhibitor is absolutely specific against its target enzyme, although both TBB and CX-4945 are highly selective against CK2 (Lolli

Fig. 6 Visualisation of Zn^{2+} under siRNA knockdown of CK2 ▶ subunit genes. Cells were treated with each specific siRNA in confocal imaging dishes for 36 h prior to $ZnSO_4$ IC_{50} treatment and confocal imaging with fluorescent probe FluoZin-3 AM (**a**). Fluorescent intensity (**b**) was quantified for each treatment with confocal images at ×40 magnification where blue indicates MCF-7 cells, orange MDA-MB-231 cells, grey PC3 cells and yellow DU145 cells. Error bars denote standard deviation of fluorescence intensity for each treatment. (Color figure online)

et al. 2012). Both TBB (20 μM) and CX-4945 (5 μM) showed the same effect, i.e. decreasing the cell viability of all four cancer cell lines under $ZnSO_4$ IC_{50} treatment (Fig. 2). Confocal imaging further demonstrates that reduction of cell viability was due to the increased accumulation of intracellular zinc (Fig. 5). These findings together indicate CK2 is involved in zinc homeostasis, potentially through regulating zinc transport proteins associated with zinc uptake, sequestration or efflux. It is well known that ZIP, ZnT and metallothioneins are the workhorses in zinc homeostasis. Zn^{2+} accumulation in breast cancer cells directly correlates with abnormal expression of ZIP6, ZIP7, ZIP10 and ZnT2 (Kagara et al. 2007; Lopez et al. 2011; Taylor et al. 2008), whilst a decrease of cytoplasmic Zn^{2+} can result from ZIP1 downregulation in prostate cancer cells (Franklin et al. 2005; Prasad et al. 2009). Further studies such as phosphoproteomics are needed to see if CK2 regulates the expression and/or activity of ZIP and ZnT.

siRNA mediated knockdown of individual CK2 subunit genes provide significant details on the involvement of CK2 in zinc homeostasis. Firstly, we analysed the efficacy of siRNA knockdown (Fig. 3). The average knockdown efficacy for all three CK2 subunit transcripts was 70.15%. Both MTT assay and confocal imaging demonstrate that CK2β knockdown is detrimental to both breast cancer cell lines whereas beneficial for both prostate cancer cell lines under IC_{50} Zn^{2+} (Figs. 4, 6). Because CK2β is essential for the tetrameric holoenzyme CK2, these findings therefore suggest that the CK2 tetramer might be involved in upregulating the cytoplasmic zinc level in prostate cancer cells, while the opposite mode of action is likely the case for breast cancer cells. The varying behaviours of breast and prostate cancer cells are also evident in siRNA knockdown of CK2α′ (Figs. 4, 6). The cell viability was reduced or zinc accumulation was elevated in PC3 and DU145 prostate cancer cells

A

| | Mock | ZnSO$_4$ IC$_{50}$ | α + ZnSO$_4$ IC$_{50}$ | α' + ZnSO$_4$ IC$_{50}$ | β + ZnSO$_4$ IC$_{50}$ |

B
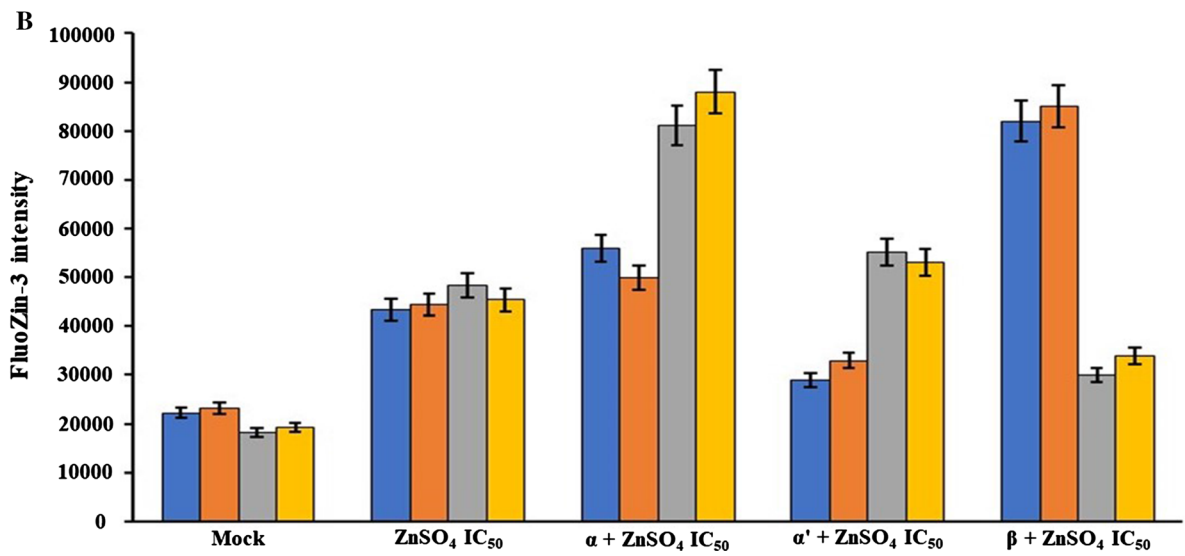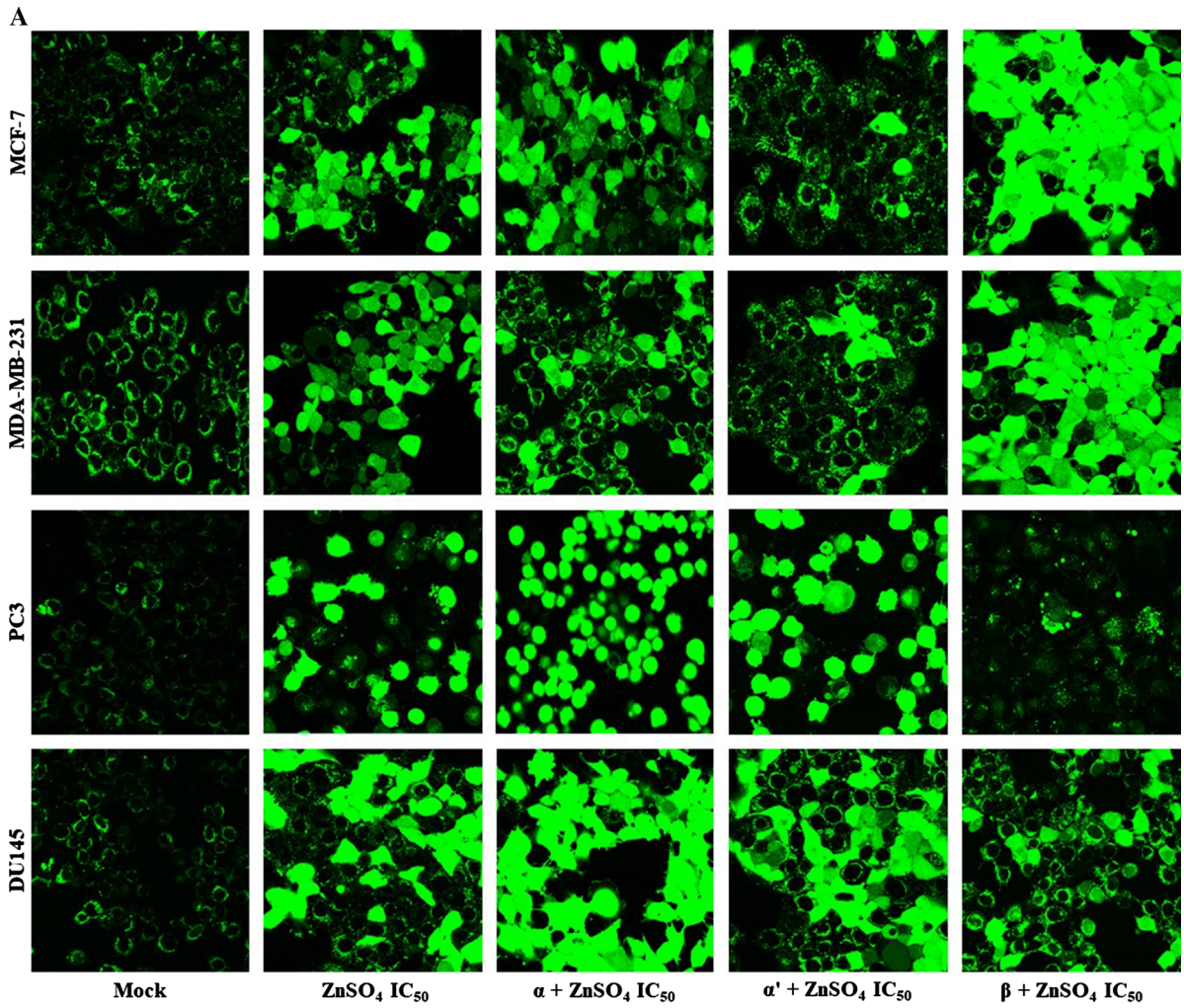
due to knockdown of CK2α′, while the opposite was seen in MCF-7 and MDA-MB-231 breast cancer cells. Such opposite effect of CK2β and CK2α′ demonstrates that CK2 is involved in zinc homeostasis, and that the CK2-related zinc homeostasis in breast and prostate cancer cells are divergent. Furthermore, siRNA knockdown of individual CK2 subunits shows that individual subunits of CK2 have distinct roles in zinc homeostasis in breast and prostate cancer cells.

In summary, the findings reported here demonstrate that CK2 is involved in zinc homeostasis in breast and prostate cancer cells, and that individual CK2 subunits play distinct roles. The study provides a basis for future works on delineating the molecular network of zinc homeostasis involving CK2, zinc transport proteins (ZIP and ZnT), metallothioneins and other players. The involvement of CK2 in zinc homeostasis may also have bearing in drug development for cancer treatment.

Author contributions MSZ Preformed all the experimental work and data analysis, and drafted the manuscript, MJW supervised the study and was a major contributor in writing the manuscript. AJJ involved in qPCR, data analysis and editing the manuscript. GP involved in qPCR and editing manuscript. GWM and QD edited the manuscript. All authors read and approved the final manuscript.

Compliance with ethical standards

Conflicts of interest The authors declare no conflicting interests.

References

Alam S, Kelleher SL (2012) Cellular mechanisms of zinc dysregulation: a perspective on zinc homeostasis as an etiological factor in the development and progression of breast cancer. Nutrients 4:875–903

Bischoff N, Olsen B, Raaf J, Bretner M, Issinger O-G, Niefind K (2011) Structure of the human protein kinase CK2 catalytic subunit CK2α′ and interaction thermodynamics with the regulatory subunit CK2β. J Mol Biol 407:1–12

Bozym RA, Thompson RB, Stoddard AK, Fierke CA (2006) Measuring picomolar intracellular exchangeable zinc in PC-12 cells using a ratiometric fluorescence biosensor. ACS Chem Biol 1:103–111

Burnett G, Kennedy EP (1954) The enzymatic phosphorylation of proteins. J Biol Chem 211:969–980

Chandler P, Kochupurakkal BS, Alam S, Richardson AL, Soybel DI, Kelleher SL (2016) Subtype-specific accumulation of intracellular zinc pools is associated with the malignant phenotype in breast cancer. Mol Cancer 15:2

Chantalat L et al (1999) Crystal structure of the human protein kinase CK2 regulatory subunit reveals its zinc finger-mediated dimerization. EMBO J 18:2930–2940

Costello LC, Franklin RB (2006) The clinical relevance of the metabolism of prostate cancer; zinc and tumor suppression: connecting the dots. Mol Cancer 5:17

Cousins RJ, Liuzzi JP, Lichten LA (2006) Mammalian zinc transport, trafficking, and signals. J Biol Chem 281:24085–24089

Cozza G et al (2009) Quinalizarin as a potent, selective and cell-permeable inhibitor of protein kinase CK2. Biochem 421:387–395

Ebert JC, Altman RB (2008) Robust recognition of zinc binding sites in proteins. Protein Sci 17:54–65

Franklin RB et al (2005) hZIP1 zinc uptake transporter down regulation and zinc depletion in prostate cancer. Mol Cancer 4:32

Guerinot ML (2000) The ZIP family of metal transporters. Biochim Biophys Acta Biomembr 1465:190–198

Guerra B, Issinger OG (1999) Protein kinase CK2 and its role in cellular proliferation, development and pathology. Electrophoresis 20:391–408

Guerra B, Boldyreff B, Sarno S, Cesaro L, Issinger OG, Pinna LA (1999) CK2: a protein kinase in need of control. Pharmacol Ther 82:303–313

Hershfinkel M, Moran A, Grossman N, Sekler I (2001) A zinc-sensing receptor triggers the release of intracellular Ca^{2+} and regulates ion transport. Proc Natl Acad Sci USA 98:11749–11754

Johnson AJ et al (2017) Unravelling the role of protein kinase CK2 in metal toxicity using gene deletion mutants. Metallomics 9:301–308

Kagara N, Tanaka N, Noguchi S, Hirano T (2007) Zinc and its transporter ZIP10 are involved in invasive behavior of breast cancer cells. Cancer Sci 98:692–697

Krężel A, Maret W (2006) Zinc-buffering capacity of a eukaryotic cell at physiological pZn. J Biol Inorg Chem 11:1049–1062

Laity JH, Lee BM, Wright PE (2001) Zinc finger proteins: new insights into structural and functional diversity. Curr Opin Struct Biol 11:39–46

Litchfield DW (2003) Protein kinase CK2: structure, regulation and role in cellular decisions of life and death. Biochem J 369:1–15

Lolli G et al (2012) Inhibition of protein kinase CK2 by flavonoids and tyrphostins. A structural insight. Biochemistry 51:6097–6107

Lopez V, Foolad F, Kelleher SL (2011) ZnT2-overexpression represses the cytotoxic effects of zinc hyper-accumulation in malignant metallothionein-null T47D breast tumor cells. Cancer Lett 304:41–51

Maret W (2001) Crosstalk of the group IIa and IIb metals calcium and zinc in cellular signaling. Proc Natl Acad Sci USA 98:12325–12327

Maret W (2012) New perspectives of zinc coordination environments in proteins. J Inorg Biocem 111:110–116

Margalioth EJ, Schenker JG, Chevion M (1983) Copper and zinc levels in normal and malignant tissues. Cancer 52:868–872

Meggio F, Pinna LA (2003) One-thousand-and-one substrates of protein kinase CK2? FASEB J 17:349–368

Meggio F, Marin O, Pinna L (1994) Substrate specificity of protein kinase CK2. Cell Mol Biol 40:401–409

Nelson N (1999) Metal ion transporters and homeostasis. EMBO J 18:4361–4371

Niefind K, Guerra B, Ermakowa I, Issinger OG (2001) Crystal structure of human protein kinase CK2: insights into basic properties of the CK2 holoenzyme. EMBO J 20:5320–5331

Outten CE, O'halloran TV (2001) Femtomolar sensitivity of metalloregulatory proteins controlling zinc homeostasis. Science 292:2488–2492

Pinna LA (1993) A historical view of protein kinase CK2. Cell Mol Biol Res 40:383–390

Prasad A, Beck F, Snell D, Kucuk O (2009) Zinc in cancer prevention. Nutr Cancer 61:879

Raaf J, Brunstein E, Issinger OG, Niefind K (2008) The interaction of CK2alpha and CK2beta, the subunits of protein kinase CK2, requires CK2beta in a preformed conformation and is enthalpically driven. Protein Sci 12:2180–2186

Schmittgen TD, Livak KJ (2008) Analyzing real-time PCR data by the comparative C T method. Nat Protoc 3:1101

Sekler I, Sensi SL, Hershfinkel M, Silverman WF (2007) Mechanism and regulation of cellular zinc transport. Mol Med 13:337

Song Y, Ho E (2009) Zinc and prostatic cancer. Curr Opin Clin Nutr Metab Care 12:640–645

Suhy DA, Simon KD, Linzer DI, O'Halloran TV (1999) Metallothionein is part of a zinc-scavenging mechanism for cell survival under conditions of extreme zinc deprivation. J Biol Chem 274:9183–9192

Taylor KM, Vichova P, Jordan N, Hiscox S, Hendley R, Nicholson RI (2008) ZIP7-mediated intracellular zinc transport contributes to aberrant growth factor signaling in antihormone-resistant breast cancer cells. Endocrinology 149:4912–4920

Taylor KM, Hiscox S, Nicholson RI, Hogstrand C, Kille P (2012) Protein kinase CK2 triggers cytosolic zinc signaling pathways by phosphorylation of zinc channel ZIP7. Sci Signal 5:ra11

Vallee BL, Auld DS (1990) Zinc coordination, function, and structure of zinc enzymes and other proteins. Biochemistry 29:5647–5659

Vinkenborg JL, Nicolson TJ, Bellomo EA, Koay MS, Rutter GA, Merkx M (2009) Genetically encoded FRET sensors to monitor intracellular Zn 2 + homeostasis. Nat Methods 6:737

Yamasaki S et al (2007) Zinc is a novel intracellular second messenger. J Cell Biol 177:637–645

Zaman MS et al (2016) Protein kinase CK2 regulates metal toxicity in neuronal cells. Metallomics 8:82–90

Zwicker F, Ebert M, Huber PE, Debus J, Weber K-J (2011) A specific inhibitor of protein kinase CK2 delays gamma-H2Ax foci removal and reduces clonogenic survival of irradiated mammalian cells. Radiat Oncol 6:15